(S) from (E). *d*) The (A) body cannot be the parent asteroid of (S) because most (A) contain abundant diopside and have negative Eu anomalies, and impact melts of (A) would not crystallize pure opx nor would they have +E anomalies. Thus, (S) probably formed on a fourth enstatite asteroid. *e*) (S) experienced a 3 stage cooling history. *Stage 1, quench:* Hundreds °/hr of (S) melt from ≥1580 °C to somewhere above 712 °C, as indicated by preservation of twinned low-Ca cpx in major opx, lack of reaction of plag, and presence of abundant Fe,Ni and FeS that did not segregate from the melt. *Stage 2, very slow cooling:* Calculations (courtesy A. D. Romig) for Fe,Ni of 9.2% Ni, 0.1% P indicate kam nucleation at 712 °C and cooling to 680 °C at < 7.5 °C/Ma. Uncertainties due to ≈ 1% Si in Fe,Ni may make this rate at most 3× faster. *Stage 3, fast cooling:* Kam-tae compositions indicate cooling rates of >0.5/day from 680–600, >0.4/day from 600–400, >0.1/day from 400–300 (in °C). *f*) This complex cooling history suggests the following origin for (S). A partly molten asteroid of nearly pure opx composition was broken up by low-velocity impact with a solid E-like object. Fragments were quenched due to incorporation of cold (>20%) projectile debris (X). That the projectile was E-like is indicated by mineral compositions and chondritic Ni/Ir [(S) 22; Hvittis 24; CI 23; $\times 10^3$]. Fragments reassembled into the (S) asteroid while T >712 °C, and deeply buried objects cooled very slowly from 712–680 °C. Excavation by impact(s) accounts for fast cooling from 680 °C. Other models not requiring break-up and reassembly are rejected because a cooling rate of ≈7.5 °C/Ma, even when assuming a lunar regolith thermal diffusivity of the ejecta blanket, requires burial at the center of a ≈14 km thick blanket. This is unrealistically thick for an asteroid-sized object.

*4.* It is unknown what caused some enstatite meteorite parent asteroids to melt (A, S), whereas others remained unmelted (EH, EL). Potential reasons may be differences in accretionary heating due to mass differences and rate of accretion, which may or may not result in sufficiently high initial temperatures conducive for melting by induction heating; or time of accretion relative to decay of $^{26}$Al.

Supported by NASA grant NAG 9-30. References: (1) Keil K. (1969) *EPSL* **7,** 243–248. Brett R. and Keil K. (1986) *EPSL* **81,** 1–6. (2) Fogel R. A. *et al.* (1988) *LPSC* **19,** 342–343. (3) Ntaflos Th. (personal communication).

**The Distribution of Trace Elements in an Allende Type B1 Inclusion.** A. K. Kennedy, J. R. Beckett and I. D. Hutcheon. Division of Geological and Planetary Sciences 170–25, Caltech, Pasadena, CA 91125 USA.

Zoning patterns of trace elements (TE) in minerals from Ca-, Al-rich inclusions (CAIs) may reflect how they formed [1] and/or yield information on secondary processes. We have measured abundances of the REE, Ba, Be, Sc and Ti in a single melilite (Mel) crystal (Xl) from the mantle of the Allende type B1 inclusion Egg-6 [2] and in the rim of a coexisting clinopyroxene (CPX) at the core/mantle interface. TE zoning profiles in Mel from Egg-6 are compared with those predicted by [1] for fractional crystallization of Mel in type B CAIs.

TE were analyzed with the Panurge ion microprobe (SIMS) using high mass resolving power (RP > 3300) for Sc and Ti and energy filtering (RP ~ 500) for all other elements. Doped Mel and CPX glasses were used as SIMS standards with sensitivity factors from [3] or based on analyses of CPX and whitlockite from Angra dos Reis. Some REE intensities were also corrected for oxide interferences [4]. Major element concentrations were determined by EDS.

The analyzed Mel Xl is normally zones from Ak33 near the outer edge of the mantle to Ak62 near the core/mantle interface. Both Ce and La concentrations rise from an initial 5× chondritic with increasing $X_{Ak}$, decrease at intermediate $X_{Ak}$, then drop precipitously to ~1× chondritic above Ak60. Ba concentrations rise with $X_{Ak}$ from 32 (Ak33) to 80 (Ak58) ppm then drop to 46 ppm (Ak62). Be (~chondritic) increases from 0.2 to 0.6 ppm over the range Ak33-Ak62 while Sc (<1 ppm) is very low for all Mel. In contrast, Ti (33–83 ppm) concentrations are highly variable and negatively correlated. Near the Mel/CPX contact, Mel is LREE enriched with a large positive Eu anomaly while CPX is LREE depleted with a negative Eu anomaly (Fig. 1). These REE patterns are similar to those for CPX and Mel separates from an Allende type B CAI [5]. If the Mel and CPX rims equilibrated with the same melt (L), then the Xl/L distribution coefficient for CPX is 5 times lower than that of Mel for Eu, 3–15 times higher for LREE and ~80 times higher for HREE. The marked decrease in Ba and REE concentrations in Mel for $X_{Ak} > 0.6$ may coincide with the appearance of CPX in the crystallization sequence. The initial rise in REE concentrations with $X_{Ak}$ was not observed by [1] in air experiments and may be due to substitution of TE on defect sites or partial re-equilibration of meteoritic Mel. Erratic Ti zoning may reflect exsolution in Mel. References: [1] Beckett J. R. *et al.* (1988) *Lunar Planet. Sci.* **19,** 49. [2] Meeker G. P. *et al.* (1983) *Geochim. Cosmochim. Acta* **47,** 707. [3] Spivack A. J. *et al.* (1988), in preparation. [4] Zinner E. and Crozaz G. (1986) *Int. J. Mass Spect. Ion Proc.* **69,** 17. [5] Mason B. and Martin P. M. (1974) *Earth Planet. Sci. Lett.* **22,** 141.

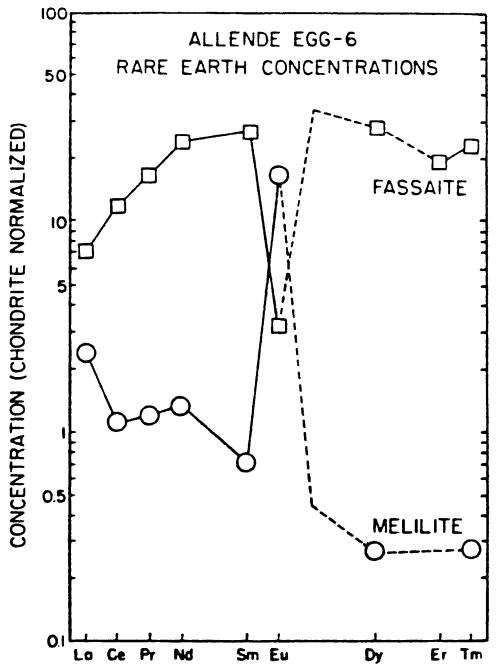


FIG. 1. REE patterns of coexisting CPX and Ak62 Mel from Egg-6.

**Djerfisherhite Compositions in EH Chondrites: A Potential Parameter to the Geochemistry of the Alkali Elements.** M. Kimura and A. El Goresy. Max-Planck-Institut f. Kernphysik, Postfach 103 980, D-6900 Heidelberg, F.R.G.

The abundance of djerfisherite in EH chondrites follows a systematic genetic pattern. It is quite abundant in the least equilibrated EH chondrites, ALHA 77295, Qingzhen, Yamato 691, and Yamato 74370. Its amount decreases to Kaidun III and St. Marks, and it is absent in Indarch and Abee. This pattern matches the subgroup arrangements of ninin-gerites [1], except for only South Oman.

The abundance of roedderite is reverse. It is highest in Indarch and decreases systematically to Qingzhen, Y-691, Y-74370, and ALHA 77295. Alkali-bearing phases in all EH chondrites include djerfisherite, caswellsilverite, roedderite, plagioclase, K-feldspar, and Na-rich glass. The assemblages, in which these phases occur, and their chemical compositions follow a distinct pattern suggestive of Na/K fractionation as a result of the condensation sequence: caswellsilverite → roedderite → plagioclase → djerfisherite. Na/Na + K ratios in djerfisherites in the EH chondrites are ordered in an array with the lowest values in Kaidun III (0.01–0.02) and Y-74370 (0.01–0.04) followed in sequence by ALHA 77295 (0.06–0.27), Qingzhen (0.12–0.17), and is highest in Y-691 (0.19–0.32). The Na/Na + K ratio in roedderite is reverse: highest in Y-74370 (0.68) and lowest in Y-691, Qingzhen, and ALHA 77295 (0.57, 0.54, and 0.56, respectively). Textures of djerfisherite-bearing assemblages in Y-74370, ALHA 77295 are suggestive of a reaction between FeNi-metal and K and $H_2O$ in solar gas [2]. Since djerfisherite and roedderite do not coexist, the observed Na/K partitioning is probably primordial resulting from the deduced condensation sequence. South Oman is enigmatic. Alkali sulfides are absent. Instead, it contains K-feldspar and plagioclase. Our investigations strongly suggest that it does not belong